

CFD Study of the Impacts of a Turbocharger's Various Wastegate and Bypass Configurations on the Efficiency and the Flow Field of its Radial Turbine

A. R. Heidary^{1†}, A. Nejat¹ and Sh. Alaviyoun²

¹ School of Mechanical Engineering, College of Engineering, University of Tehran, Tehran, Iran

² Air Charging System Department, RISECO Holding, Tehran, Iran

†Corresponding Author Email: amir.r.heidary@ut.ac.ir

(Received August 16, 2022; accepted February 1, 2023)

ABSTRACT

Turbocharger systems enhance the engine power and efficiency, reduce its pollution, and downsize the engine volume. As the significance of exploiting turbochargers in gasoline engines is surging among automobile manufacturers, the necessity of improvement in the system components becomes more critical. This paper investigates the impacts of a turbocharger turbine bypass and wastegate geometry alterations on the performance and the flow field characteristics via numerical simulations. The numerical method verification and mesh independence study are performed for the original geometry. The simulation results of the altered geometries indicate that better alignment between the bypassed and the bulk flows leads to higher efficiency of the turbocharging system. In addition, the bent or elbow-shaped and protruded turbine walls immediately downstream of the wheel are found to be unfavorable. It is also uncovered that if the wastegate shape and the housing walls are designed in such a way that the effects of ensuing vortices are minimized, it improves the stage efficiency, which is desirable for two-stage turbochargers. Furthermore, a novel manufacturable design is proposed in this study, which increases the efficiency and useful power by 19.9% and 6.7%, respectively.

Keywords: Optimizing; Turbocharger turbine; Geometry alterations; Simulations; Computational fluid dynamics.

NOMENCLATURE

A/R	area over radius	T	turbine wheel torque
ER	Expansion Ratio	$Y+$	dimensionless wall distance
H_0	total enthalpy	ω	angular velocity
P_{total}	total lost power	η	efficiency
P_{useful}	useful power		

1. INTRODUCTION

Thanks to rigorous emission regulations and fuel economy standards set by governments around the world, boosting and downsizing are the global trend of gasoline engine technology. Therefore, automobile manufacturers refine the fuel efficiency, power output, and emission control of their vehicles' engines. One proven and reliable approach is to exploit turbocharging technology which does not sacrifice drivability nor does add significant up-front costs (Gao *et al.* 2016).

A turbocharger primarily encompasses a centrifugal compressor and a radial turbine. Those are connected by a common shaft which is supported via a central

bearing housing whose other duty is lubricating the rotating shaft. The high energy of the engine exhaust gas is extracted by the turbine and then delivered to the compressor through the rotating shaft. The compressor, subsequently, increases the density of the entering ambient air (which passes a filter prior to entering the compressor). As a result, the oxygen level, required for combustion, rises. The intercooler, which is placed between the compressor and the engine, further contributes to density rise by reducing the temperature of the compressed air flow. Therefore, the combustion in the engine cylinder occurs in higher pressure with more oxygen (and a bit more injected fuel) producing more power and torque. Consequently, to provide the same amount of

power, a turbocharged engine has smaller displacement, less mechanical losses, weight, and squandered energy than a naturally aspirated one (Fogarty 2013). The turbine's useful power depends on the Expansion Ratio (ER), which is the ratio of the wheel inlet pressure to its outlet pressure, and a higher ER is desired for higher generated power. (Baines 2005).

Although turbochargers have been utilized in diesel engines for decades, their prevalence in gasoline engines does not have such a long history. This mainly derives from the fact that the gasoline engines' working range is much wider than that of diesel engines. That poses a few challenges such as more elevated exhaust gas temperature, a broader range of flow rates, and complicated boost pressure controlling system. At a low engine speed, the available exhaust energy can provide enough torque for the compressor (employing a small turbine wheel) to boost the inlet engine pressure without a sizeable turbo lag. As the engine speed increases, so does the exhaust temperature and pressure leading to the turbine wheel's over speed, excessive boost pressure, and engine knock. In order to avoid this deleterious effect, it is imperative to use a large wheel turbine instead of a small one. The downside of a large wheel turbine, however, is the increased turbo lag. Thus, the conventional fixed geometry turbines can only be matched with either a low, medium, or high engine speed. Employing adjustable turbines addresses the problem and is under rapid development (Chen *et al.* 2016).

So far, two general types of adjustable turbines have been developed; 1) Variable Nozzle Turbines, also known as Variable Geometry Turbines (VGT), and 2) Wastegated Turbines. Regarding manufacturing complexity, the latter technology is less complicated and therefore it is more common. In this technology, the wastegate valve head is controlled by either an electric (which gets its command from the Electronic Control Unit (ECU)) or via a pneumatic actuator (which might be connected to the compressor housing). Although the electric actuator is more complex and expensive, it is more precise and responds to the changes faster (Fogarty 2013; Chen *et al.* 2016). In wastegated turbochargers, the performance of the turbine highly hangs on the wastegate position as it controls the boost pressure. Under wastegate-closed and part-load engine conditions, the turbine conforms to its characteristic map (Hiereth and Prenninger 2007) and the efficiency reaches to its maximum amounts. However, the opening of the wastegate valve reduces the turbine efficiency since a proportion of the exhaust gas is bypassed and its energy is wasted and not handed to the wheel (Marelli and Capobianco 2011; Salim 2014).

To investigate the performance of the wastegated turbochargers turbines, several studies were conducted. Salehi *et al.* (2013) performed a 0-D simulation in which the turbine was modeled as an isentropic nozzle and the wastegate as an orifice. Mousavi *et al.* (2021) worked on an integrated 0-D turbocharger and engine simulation program with engine details in which a quasi-steady compressible

flow approach is employed. This model gives the performances of various turbine-compressor combinations in a combustion engine. Serrano *et al.* (2017) developed an approach for the discharge coefficient characterization of a wastegate valve. The discharge coefficient map was created after the 1-D gas model and empirical data correlation and validation were done. In another study by Chen *et al.* (2016), it was ascertained that the wastegate diameter has a considerable impact on the turbocharged gasoline engine performance. The full opening of the wastegate under small and medium loads can ameliorate both the engine power output and fuel economy. As the engine load increases, so do the air intake requirements. In order to gain adequate boost pressure, the optimal wastegate opening shrinks. The lower the engine speed is, the smaller the wastegate opening needs to be set, so as to attain the best engine performance. Although 0-D and 1-D models provide us with fast and acceptable predictions, they are not able to present details of the flow field in turbines.

The three-dimensional fluid flow in a turbocharger is a complex turbulent flow including backflow structures and vortices. CFD is, therefore, a powerful tool to study and scrutinize fluid fields in turbocharger turbines and has been utilized by many researchers e.g. Capiluppi (2012) and Benajes *et al.* (2014). Single Blade Passage (SBP), as well as the Full Turbine (FT) approaches make up the two common 3-D simulation methods. In the former, the flow inside one passage of the blade is simulated and the set periodic surfaces are representative of the rest of the domain (Shah *et al.* 2016). The latter method is a much more authentic approach as it models the whole turbine, providing the flow field across the rotor, stator, and the volute (Siggeirsson and Gunnarsson 2015). In the study conducted by Tabatabaei *et al.* (2012), it was shown that in both steady-state and transient flows (wastegate-closed condition), increasing engine speed is followed by reducing simulation errors.

Numerous studies have investigated the turbocharger turbine flow field under steady-state conditions and provided scholars with valuable and helpful results. Despite that, internal combustion engine exhaust gases have a pulsating flow nature which causes unsteady behavior of the turbine stage. Rezk *et al.* (2021) presented the realistic effects of the pulsating flow of different characteristics on the performance of a radial turbine by coupling a 3-D CFD model with a 1-D engine model. Also, Mosca *et al.* (2021) used unsteady CFD to study the effects of the parameterized characteristics of the mass flow pulse. From that work, pulse amplitude is discovered to be the main parameter that affects turbine performance, heat transfer, and entropy generation.

The numerical study performed by Getzlaff *et al.* (2010) showed that the bypassed exhaust gas flow velocity can increase up to 800 m/s at the wastegate channel because of its narrowing cross-sectional area. According to another study carried out by Hasler (2018), if the bypassed flow is not directed correctly, it causes high mixing losses. From this study, it was concluded that, instead of the

conventional baseline design, the separated bypass design can be used so as to increase the stage efficiency. In the latter designing method, the angle at which the bypass flow rejoins the bulk flow (the mixing angle) is a pivotal factor in determining the stage efficiency.

In a recent numerical study, which was also validated experimentally, [Alaviyoun *et al.* \(2020\)](#) showed that as the gasoline engine speed goes up, so does the bypass flow ratio (The ratio of the wastegate flow to the turbine total flow). Furthermore, they detected unfavorable turbine back-pressure as well as high mixing losses from the streamlines. They were primarily caused by the unparallelled direction of the wastegate passage and the turbine centerline and they were elevated as the wastegate opening angle was increased. A remarkable result of their research is the 80 kPa pressure difference between two sides of the wastegate valve (at 2 degrees opening angle). Due to this difference and nonsymmetrical pressure distribution, the valve instabilities and controllability become serious issues.

Apart from the bypass design and wastegate diameter, the shape of the wastegate valve can also influence the performance of the turbocharging system. Changing the flat wastegate valve surface to a new version with a spheroid protrusion in CFD simulations and on cold flow bench tests performed by [Dupuis *et al.* \(2014\)](#) showed that by increasing the wastegate valve opening angle from 0 to 30 degrees, a smoother rising mass flow as well as load decrease and lower arm torques were achieved. This achievement was asserted to have enriched the valve controllability drastically, particularly in the nearly closed position.

Another innovative approach for optimizing turbochargers having bypass flow is the work done by [Steglich *et al.* \(2020\)](#). In this study, the wastegate system is replaced by a jet pump nozzle working based on the momentum exchange between driving and suction flows. The fluid jet accelerates the suction flow and it drops the static pressure in the suction pipe. Therefore, the pressure gradient between the turbine wheel inlet and the nozzle outlet forces a part of the inlet flow to pass the wheel. The upsides of this technology were listed as; 1) 20% higher turbine output power, 2) 7% higher efficiency, 3) 8% lower effective specific fuel consumption, and 4) refined transient engine operation. Moreover, they proposed another configuration for the system. In that configuration, an adjustable aerospike nozzle with a changing cross-section, is utilized instead of the fixed jet pump nozzle. This led to reduced mixing effects where the two separated flows meet, reducing the flow losses.

In addition to numerical simulations, sophisticated experimental investigations are pursued as well. Optical measurement techniques were employed by [Wibmer *et al.* \(2015\)](#) to video-image the complicated bypassed flow of the wastegated turbochargers. In addition, [Fogarty \(2013\)](#) experimentally investigated the steady flows of three different wastegated turbochargers of varying turbine/wastegate combinations i.e. two of similar turbine housing

(BorgWarner) but different bypass throat diameters, and a third of both different housing (Honeywell) and throat size from the former ones. They performed the experiments on a cold-flow turbocharger test bench; The Honeywell turbine passages resemble a typical tee junction, whereas the BorgWarner bypass port utilizes a half-bowl-shaped depression to connect the wastegate throat to the inlet passage. The effects of that design difference include greater wastegate-alone flow efficiency for the Honeywell at the maximum opening (40°).

Regarding 2-stage turbochargers that are prevailing in internal combustion engines, when the wastegate valve of the first stage is open, the interaction of the swirling flow exiting the turbine wheel with the bypassed one results in strong secondary flow, distorting the inlet flow condition for the rotor and leading to more entropy generation in the low-pressure turbine and hence decreasing the second stage efficiency ([Yang *et al.* \(2021\)](#)). That indicates the significance of the design of the first-stage housing.

In respect of twin-entry turbines, the results of the study conducted by [Hajilouy *et al.* \(2009\)](#) show that the distortion near the tongue of the volute, where there is a complex 3-D flow field, gives the lowest gain factor of entropy. The shear layer, which is shaped between the flowing and stationary regions in the mentioned area, causes the most entropy generation in the turbine ([Newton *et al.* \(2012\)](#)). [Galindo *et al.* \(2022\)](#) suggested that two things should be considered in mean line loss-based models for their importance in unequal admission conditions; (1) Flow branches of a twin-entry turbine are not fully combined with one another within the rotor, and (2) the momentum exchange between flow branches causes losses in the contact region.

The chief aim of this article is to propose a novel and refined manufacturable design for the original turbocharger turbine used in the study worked on by [Alaviyoun *et al.* \(2020\)](#), by changing its bypass passage, turbine walls, and wastegate shapes. The numerical procedure is validated by the experimental results of the original study. Diverse generated geometries in this paper are inspired by the obtained experiences from previous studies and finally, a new combined design is suggested. Steady-state CFD simulations are applied to all the aforementioned design concepts at the same working point where the maximum opening angle of the wastegate valve and the lowest efficiency of the original turbine occur. The goal is to compare the useful power and the efficiency of the different configurations and to clarify the underlying reasons why a design surpasses others.

2. MATHEMATICAL MODELS

A RANS (Reynolds-Averaged Navier-Stokes) flow solver of a commercial software, ANSYS Fluent 2022 R1, is used for coupled compressible flow simulation. Due to the fact that we are dealing with a steady-state multiple-zone problem (in which there are stationary and rotating fluid zones), it is reasonable that we employ Multiple Reference

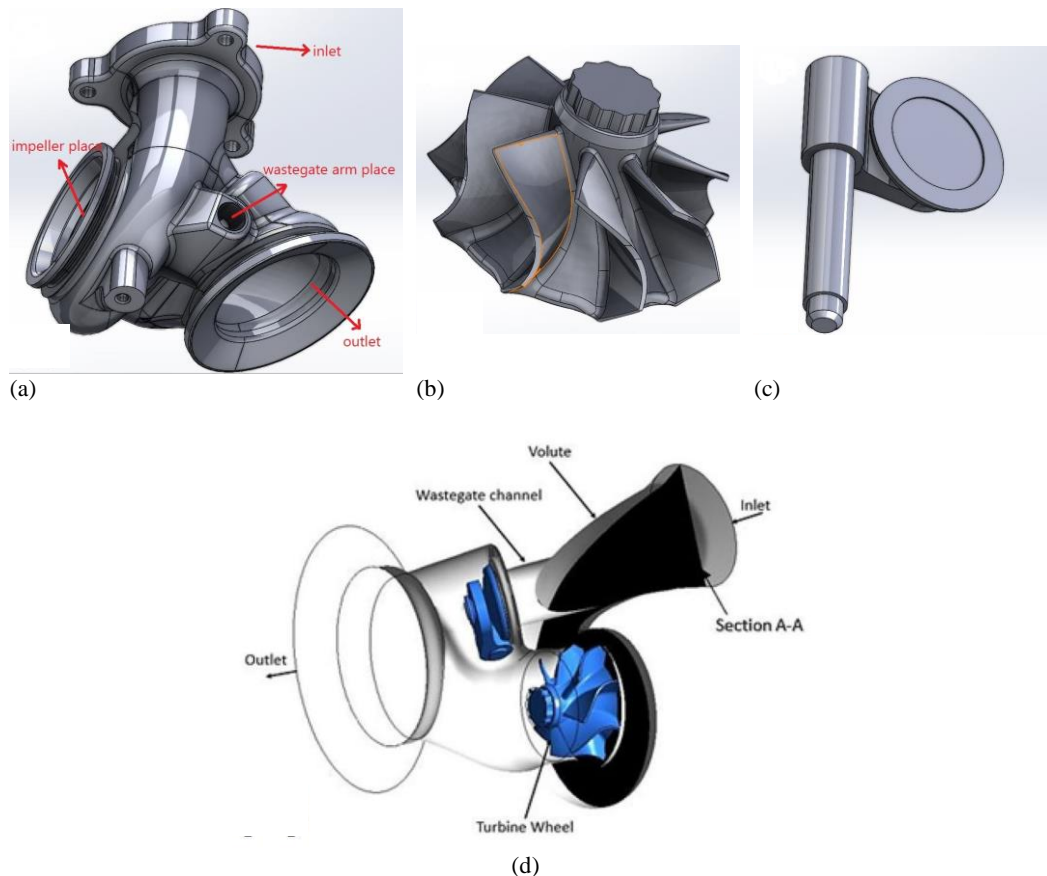


Fig. 1. Parts of the original geometry (a) Turbine housing, (b) Impeller (turbine wheel), (c) Wastegate arm and valve, (d) An assembled model.

Frame (MRF) model which considerably cuts down on computation time. In this approximation for the rotating zone, there are additional terms in the momentum equation which account for the Coriolis and centrifugal accelerations since a coordinate system rotates with the rotating zone. This is while the grid is fixed and there is no relative motion between the two zones as though the rotor is frozen, which is why this model is also referred to as the Frozen Rotor Approach. It is also noticeable that in this approach, the flow properties are directly translated at the common interface of the mentioned zones. More information about equations and the solver can be found in the article by [Alaviyoun *et al.* \(2022\)](#) and section 3.3 of the current study.

3. SIMULATION STEPS

3.1 Geometries

The original turbocharger turbine that is used for the Grid Independence and the Numerical Method Validation sections of this paper has the specifications shown in Table 1. Also, different parts of the turbocharger are shown in Fig. 1.

A/R, which stands for Area over Radius, is defined as the inlet cross-sectional area divided by the distance from the turbo centerline to that area's centroid ([Hiereth and Prenninger 2007](#)). A pressurized actuator system is utilized to open the normally-closed wastegate that can be opened only

Table 1 Original turbine specifications.

Geometrical Features	Value
Turbine housing A/R	0.5
Turbine inlet diameter	39 mm
Turbine outlet diameter	60.64 mm
Impeller inducer diameter	43.6 mm
Impeller blades number	8
Maximum tip speed	502 m/s
Wastegate passage diameter	20 mm
Wastegate valve diameter	27 mm

up to 7 degrees. The main parts of the model are depicted in the following picture.

By pursuing a set of commands in CAD software (SOLIDWORKS in this study), one can extract the negative volume of the solid parts shown above. This negative volume represents the fluid domain that is to be set as the fluid zone in simulations. Figure 2 illustrates the whole fluid domain and a sectioned view of it. Notice that the extended outlet is 10 times longer than the impeller diameter to avoid reverse flow ([Capiluppi 2012](#)). In this geometry, the angle between the bypass duct centerline and the impeller axis is 25 degrees.

Alongside the original geometry, which has a so-called baseline design, are the separated design, jet pump nozzle concept, and the suggested improved

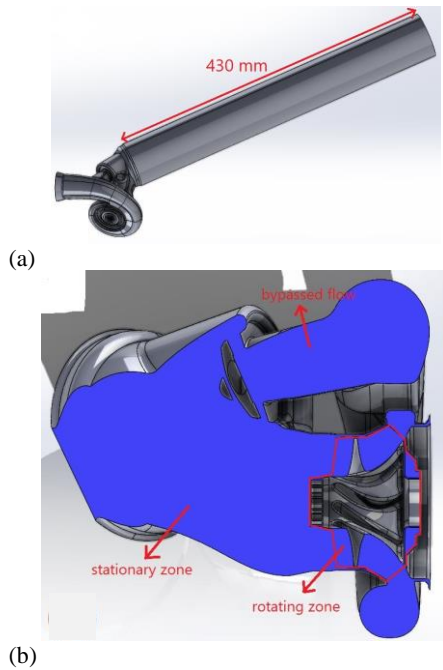


Fig. 2. Fluid domain of the original geometry
 (a) The whole fluid domain, (b) Sectioned view of the fluid domain.

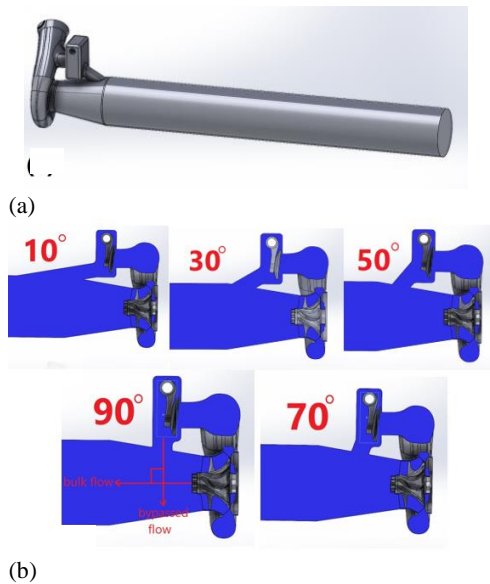


Fig. 3. Separated design
 (a) 3D view of a separated design, (b) Different mixing angles.

models. The separated design geometries that are shown in Fig. 3 are created for 5 mixing angles (the angle at which the bulk flow exiting the turbine wheel is reintroduced to the bypassed flow).

The two jet pump nozzle geometries are also shown in Fig. 4. As can be seen, the nozzle can be either fixed or adjustable. In the latter concept, the cross-sectional area of the nozzle is changed by the movement of the central aerospike-shaped piece.

Although the above offered concepts might sharpen the flow field and the efficiency of the turbine housing, their production is still a challenge because

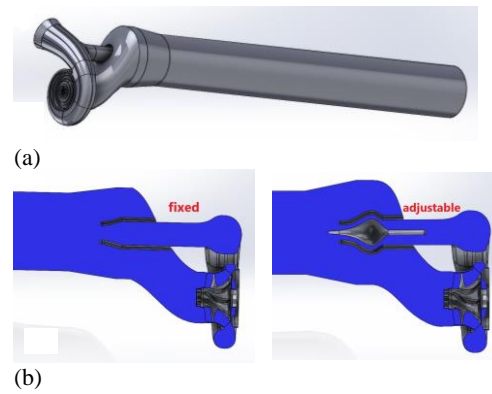


Fig. 4. Jet pump nozzle design
 (a) 3D view of a jet pump nozzle design, (b) Sectioned views of fixed and adjustable nozzles.

of their complexity and limitations of packing as well as manufacturing such as the need for machining the wastegate flap seat. Furthermore, one discernible downside of the jet pump nozzle is the turbo lag as it takes some time for the wheel to start rotating in the beginning of the vehicle movement. Therefore, we have developed another novel concept which lacks turbo lag, is manufacturable and somehow a combination of the separated and baseline designs. This is shown in Fig. 5. As can be observed, there is a wall acting as an obstacle not allowing the bypassed flow to directly join the bulk flow of the turbine. The bypass duct centerline and the impeller axis are parallel as well. Also, pay attention that the cross-sectional area of the bulk flow increases from the wheel outlet to where the two separated flows join (like an oval-circular cylinder).

In order to investigate how the wastegate valve might affect the flow field, the efficiency, etc. its shape had to be modified in such a way that the flat flap was replaced by a spheroid protrusion and a few sharp edges got replaced with fillets. Figure 6 shows the differences between the original and modified

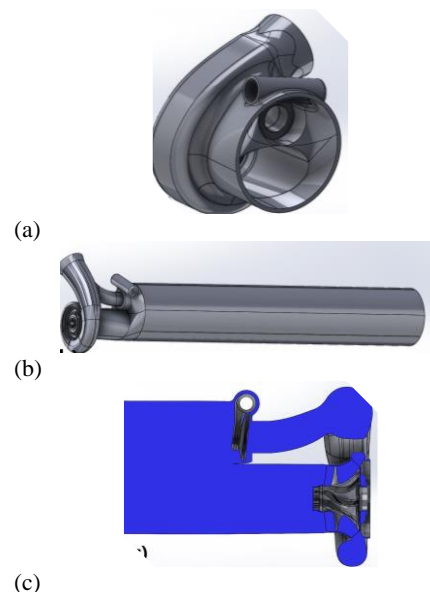


Fig. 5. Combined design different views
 (a) Prototype housing, (b) Fluid domain, (c) Sectioned view.

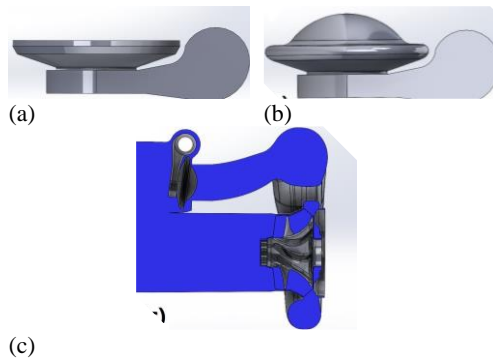


Fig. 6. New wastegate
(a) Original wastegate, (b) Modified wastegate,
(c) Sectioned view of the combined design with
the new wastegate.

wastegates as well as the sectioned view of the combined design with the new wastegate valve.

Finally, notice that the volute, turbine wheel, bypass duct diameter, and the outlet diameter of all the geometries are not changed (only the outlet diameter of the combined design had to be increased by 0.6 cm because of its configuration).

3.2 Mesh

Because of the geometry complexity, the computational grid is mainly comprised of unstructured tetrahedral mesh with inflation layers near walls. The height of the first boundary layer should be chosen in regard of the turbulence model so that an acceptable dimensionless wall distance of Y^+ is realized. For instance, if the k- ω SST turbulence model is selected, a much refined mesh should be generated to achieve a Y^+ value close to 1 (Galindo *et al.* 2013), which results in a computationally expensive simulation. On the other hand, some other models such as k-epsilon model require a Y^+ value less than 10 on the rotor walls (Cox 2015). A computational grid as a sample is shown in Fig. 7. In ANSYS, a conformal mesh on the interfaces can be easily obtained in Meshing by forming 1 multi-body part in Design Modeler prior to importing the geometry to Meshing. Considering mesh quality, the closer Skewness to 0 and the closer Orthogonal Quality to 1, the better. Skewness amounts of over 0.94 and Orthogonal Quality amounts of below 0.15 will most likely cause errors in the next steps. More information on mesh is available in the Grid Independence section of this paper.

3.3 Computational Setup

An indispensable step of any numerical study is the realistic selection of boundary conditions. The boundary conditions of the current study are the empirical results of the experiments carried out by Alaviyoun *et al.* (2020, 2022). Steady-state experiments at various engine speeds and full load conditions were performed on a standard gasoline engine test bench and many parameters like temperature, pressure, impeller rotational speed, gas mass flow rate, etc. were measured. The whole

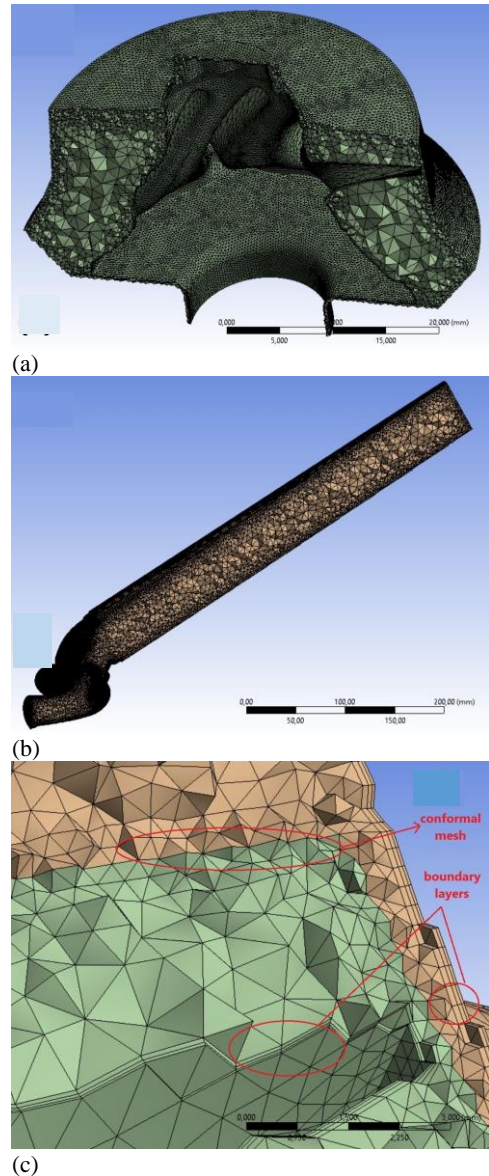


Fig. 7. Mesh
(a) Rotating domain, (b) Stationary domain, (c)
Boundary layers and conformal mesh.

procedure of sensors installation and measurements is explained in the mentioned papers and the results of 3 working points under full load conditions are listed in Table 2.

In the real case scenario, all the heat transfer mechanisms occur between the turbine housing and its environment, namely the convection heat transfer between the housing and the ambient air with different coefficients in different parts of the turbine, conduction heat transfers between the inlet flange and the exhaust manifold of the engine as well as the turbine housing and the bearing housing, radiation heat transfer between the exhaust manifold and the housing, and finally the internal convection heat transfer between the turbine housing and the gas. However, setting the mentioned conditions in a precise way is complicated and time-consuming. Due to this fact and the main goal of this study which

Table 2 Boundary conditions.

Working Point	1	2	3
Impeller rotational speed (rpm)	92000	142000	168000
Inlet total pressure (kPa)	30.5	100.2	207
Inlet total temperature (K)	1087	1156	1214.4
Outlet gauge static pressure (kPa)	3.1	16.8	48
Outlet total temperature (K)	972	1019	1084
Wastegate opening angle (degrees)	0	2	7

is to compare disparate configurations at the same working point and boundary conditions, it was decided that only the fluid domain be modeled and the thermal boundary conditions on all the walls be set to constant temperature walls (except the impeller, heatshield, and outlet extended walls that are adiabatic walls). From the experiments, it was found that the average temperature of the internal walls is in the range of 200 to 250 Kelvin less than the inlet total temperature. Also, all the walls have the no-slip shear condition and are stationary apart from the impeller wall that is a moving wall with a rotational speed of 0 rpm relative to the rotating zone.

Although the real fluid of the problem is a burnt blend of air and gasoline and mostly made up of carbon dioxide (CO₂), nitrogen gas, and water vapor (meaning that the Species Transport model should be activated), for convenience and reducing the computation time, the modeled gas is chosen to be an ideal gas defined by the Piecewise-polynomial approach for the specific heat capacity, Piecewise-linear for thermal conductivity, Sutherland for viscosity, Ideal-gas for density, and constant molecular weight of 29 kg/kmol.

The simulations were run using the pressure-based solver with the coupled scheme, which obtains a robust and efficient single-phase implementation for steady-state flows, alongside distance-based Rhie-Chow flux type. Since the convergence and the stability of the 2nd order upwind spatial discretization of the equations were so demanding that it consumed too much time and there was not a substantial difference between its results and those of the first order upwind discretization as it was observed (less than 2%), the first order upwind discretization was used for the main equations. Least Squares Cell Based and Standard discretization types were utilized for Gradient and Pressure, as well.

In regard to the turbulence model, it is essential to maintain Y^+ close to 1 if the k-w SST model is employed. In order to do this, the boundary layer first cell height must be decreased significantly which culminates in a computationally costly simulation.

This is while its results differ approximately 1 percent from those of the k-epsilon model for the prediction of turbine performance (Alaviyoun *et al.* 2022). Nevertheless, the reliable k-w SST model was exploited, as it was chosen in many previous studies.

Additionally, it is noticeable that there is no need to define an interface in the commercial CFD software (ANSYS Fluent in this study) on the common faces of the rotating and stationary zones as there is no mesh motion in MRF approach and the mesh is conformal on those faces.

For initialization, the Full Multi-Grid (FMG) method, in which the inviscid Euler equations are solved using 1st order-discretization, was used after a Hybrid initialization. This provides us with the best initial values for our case since we are facing a turbomachinery problem with a compressible fluid. The solution, finally, is considered to be converged once all the residuals have dropped at least by 4 orders and the monitored outputs, in particular inlet mass flow rate, outlet velocity magnitude and static temperature, and turbine wheel torque remain unchanged in the new iterations.

4. SIMULATION RESULTS AND DISCUSSION

4.1 Grid Independence

To reach the appropriate mesh size for the simulation, a mesh independence study was conducted based on the gas mass flow rate and the impeller torque. From Fig. 8, it is quite clear that the mesh with 4.7 million elements is good enough for the independency of the results since by employing the finer mesh no remarkable change in the simulation outcome is observed (Table 3).

Table 3 Mesh results

	Relative Difference Between #1 and #2	Relative Difference Between #1 and #3
Torque	0.15%	0.06%
Mass Flow Rate	0.16%	0.20%

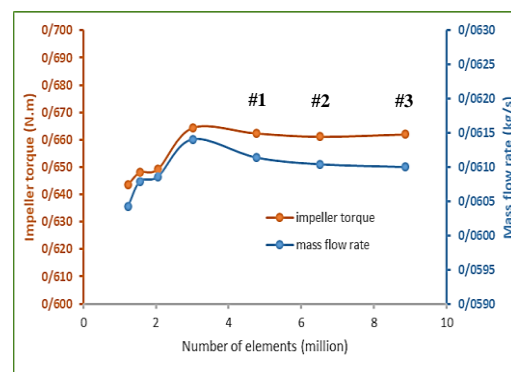


Fig. 8. Mesh independence.

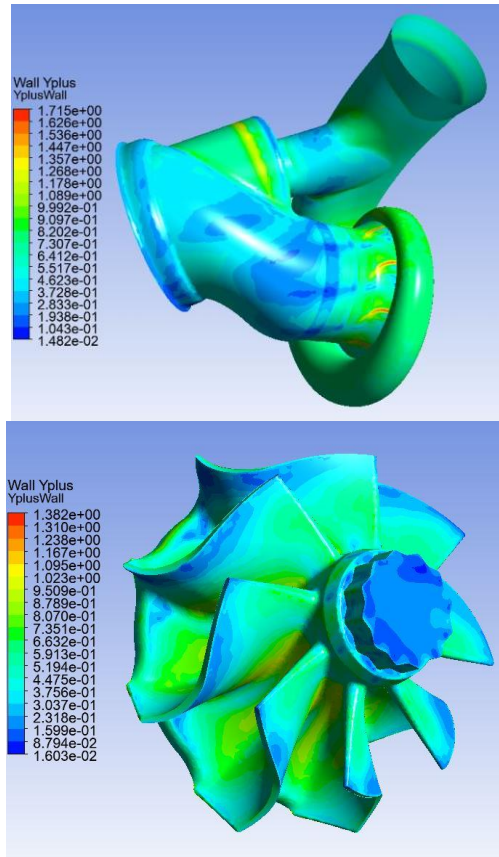


Fig. 9. Y+ distribution on the walls of the turbine housing and the impeller.

4.2 Numerical Method Validation

In all the simulations, since the k-w SST turbulence model was selected, the prism layer was refined until a Y+ very close to 1 was realized so as to properly capture the viscous boundary layer and guarantee an adequate resolution of the temperature gradient. Figure 9 exhibits the Y+ distribution on the walls of the turbine housing and the impeller in one of the cases with the maximum amount of 1.715.

Working points 1 and 2 were chosen for the model verification. Table 4 depicts the deviation of the calculated parameters from the measured experimental results. Notice that the Outlet gas temp. is the static temperature of the gas at the turbine outlet and the points P1 and P2 on the turbine housing are shown in Fig. 10.

Notwithstanding the discrepancies seeming to be glaring at first glance, they are, in fact, reasonable. For the reasons that our prime goal was limited to the scrutiny of how geometry alterations (under the same boundary conditions) might influence the results and there were too many cases to be simulated, it was decided that the thermal boundary conditions be simplified as much as possible (constant temperature turbine walls, as it was explained earlier), and the Species Transport model remain deactivated. Even though these two decisions greatly contributed to shortening computational time, they are the primary causes of the errors. Additionally, a high percentage of the mentioned errors originates from

Table 4 Comparison of numerical and experimental results (white: working point 1, Blue: working point 2)

	Experiment	Simulation	Prediction error (%)
Mass flow rate (kg/s)	0.02822	0.02963	5.00
	0.05812	0.061	4.96
Outlet gas temp. (K)	956	1013.09	5.97
	1023	1085.61	6.12
Pressure @ P1 (kPa)	26.23	24.7	5.83
	89.19	83.552	6.32
Pressure @ P3 (kPa)	23.41	21.93	6.32
	75.12	70.087	6.70

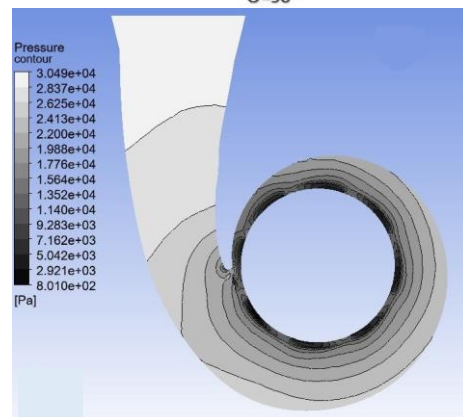
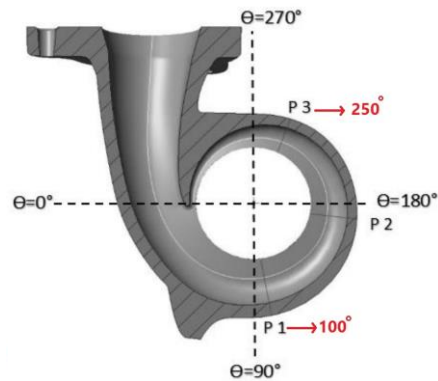


Fig. 10. Pressure sensor positions and pressure contour in a sectioned view (a) Sensor positions, (b) Pressure contour.

the geometrical simplification of some parts such as the heatshield and wastegate, plus the potential imprecise longitudinal location of the impeller when the system was assembled in the CAD software (this longitudinal location is the same for all the geometries). Had the real thermal boundary conditions been set by Conjugate Heat Transfer simulation, the Species Transport model been activated, and the CAD geometry been modeled more precisely, the errors would have decreased to less than 5% (Alaviyoun *et al.* 2020, 2022). The

discretization method, MRF approach, turbulence model, and the experiments uncertainties make up the left proportion of the error sources.

4.3 Useful Power, Efficiency, and the Flow Field

In the original geometry, as the opening angle of the wastegate valve rises, so do the mixing losses (Alaviyoun *et al.* 2020). This is why working point 3 (at which the maximum opening angle occurs because of the geometrical limitations) was selected as the most critical condition for comparing the generated geometries. Figure 11 shows the preliminary results of the computational study. The turbine wheel torque (T), inlet and outlet total enthalpy (H_0) can be directly calculated using CFD post-processing. Subsequently, the useful power (power extracted by the impeller), total power that is lost in the whole system, and turbine stage efficiency can be obtained by the following equations (ω and η represent the rotational speed and efficiency, respectively).

$$P_{useful} = T \times \omega \quad (1)$$

$$P_{total} = H_{0,inlet} - H_{0,outlet} \quad (2)$$

$$\eta = \frac{P_{useful}}{P_{total}} \quad (3)$$

As can be ascertained from Fig. 11, the original design and combined design seem to be the best and the worst ones in respect of the efficiency with a 19.9% relative difference. The static pressure and velocity contours alongside the streamlines of these cases can be of great use for us to uncover the underlying causes of their being the least and the most promising designs.

What can be perceived from the aforementioned figures is that in the original baseline design, the high-speed bypassed gas jet acts as if there is a wall

blocking the progression of the bulk flow immediately downstream of the wheel. This aerodynamic blockage causes the average static pressure at the wheel outlet to increase, which culminates in a decline in the Expansion Ratio (ER) across the turbine wheel as the turbine's inlet pressure remains unchanged. The available energy that is to be extracted by the wheel, consequently, decreases (less useful power). Identically, a part of the housing in the original design resembles an elbow that diverts the bulk flow and causes stagnation, which boosts the average static pressure at the impeller outlet, causing the ER and useful power to go down. In contrast, in the combined design, the mixing losses are considerably less than that of the former design owing to the bypassed flow reintroduction method which does not allow the bypassed high-velocity jet to perpendicularly disrupt the bulk flow, and there is no sign of the mentioned back pressure caused by the housing elbow-shaped walls. Notice that the pressure contours shown in Fig. 15 are created only for the static pressure field downstream of the wheel and wastegate so as to better show what was explained.

Furthermore, vortices and swirls produce losses which result in more fall in the total enthalpy and hence the turbine stage efficiency. These phenomena sound to be more prevalent in the combined design in comparison with the original one. However, the shape of the housing around the wastegate is more of a fluke, knocking down the kinetic energy of the streamlines that travel around the wastegate arm. Therefore, the effects of those phenomena in this design are not as adverse as those of the baseline configuration. This can be concluded from the color of the streamlines in Fig. 13.

Comparing geometries number 9 and 10 from Fig. 11, while the efficiency of the system using the new wastegate is slightly more, its useful power is negligibly less. The former can be justified considering the fact that some of the sharp edges and blunt bodies of the wastegate were replaced by curvy shapes which de-escalate the associated vorticity losses.

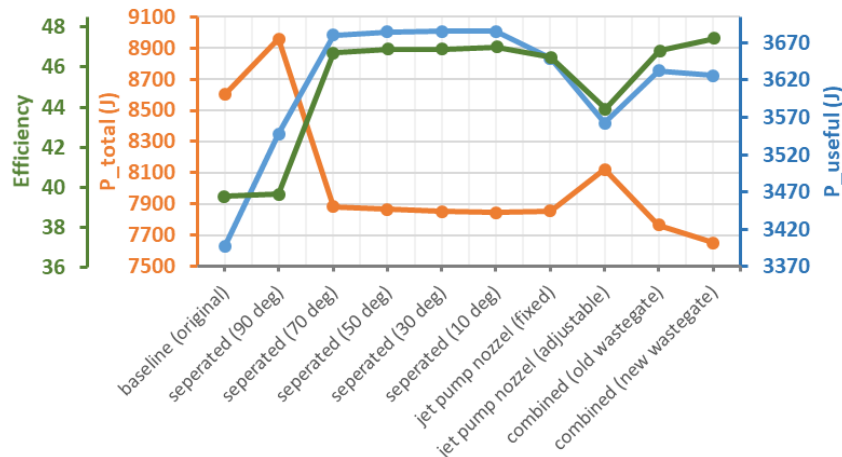


Fig. 11. Results of the computational study on the geometries at working point 3.

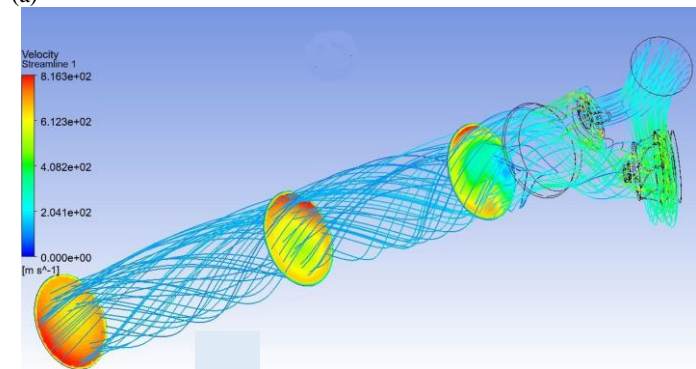
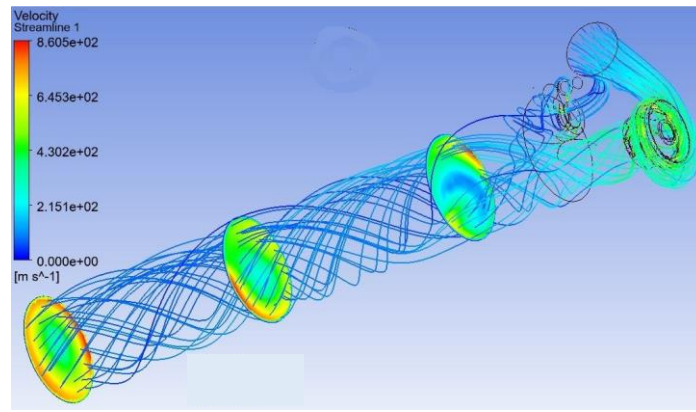


Fig. 12. 3-D stream lines with local velocity contours (a) Combined design, (b) Original design.

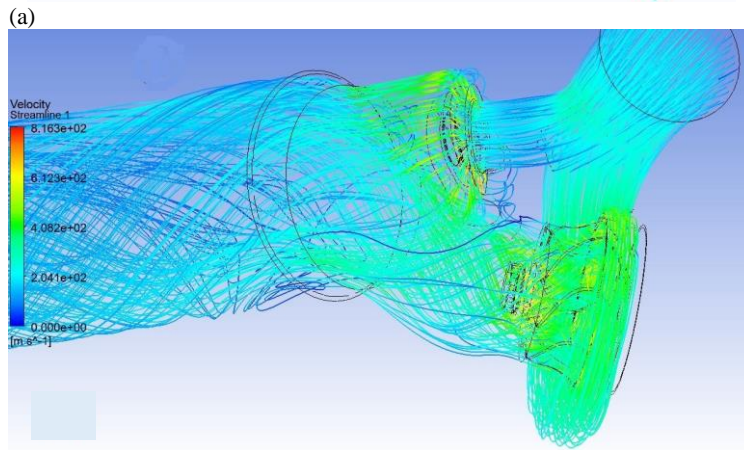
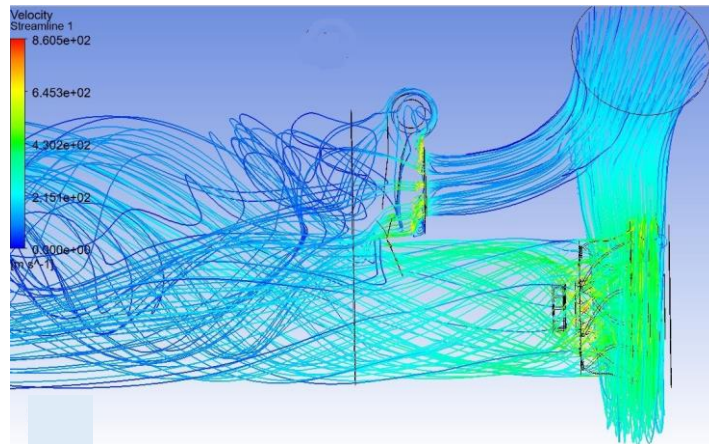


Fig. 13. Closer look at the stream lines of the housings (a) Combined Design, (b) Original design.

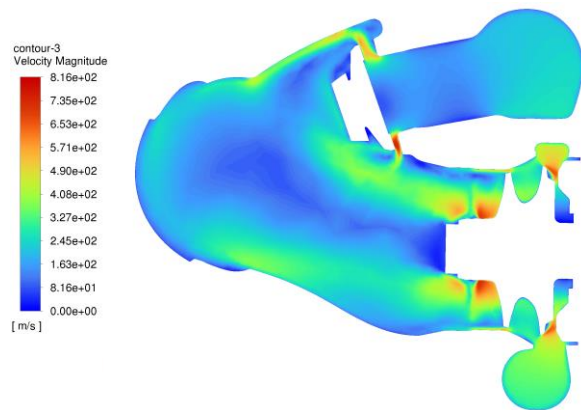
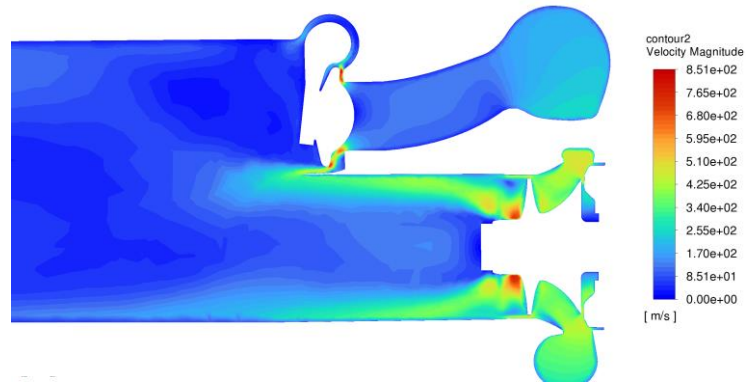


Fig. 14. 2-D velocity contours (a) Combined Design, (b) Original design.

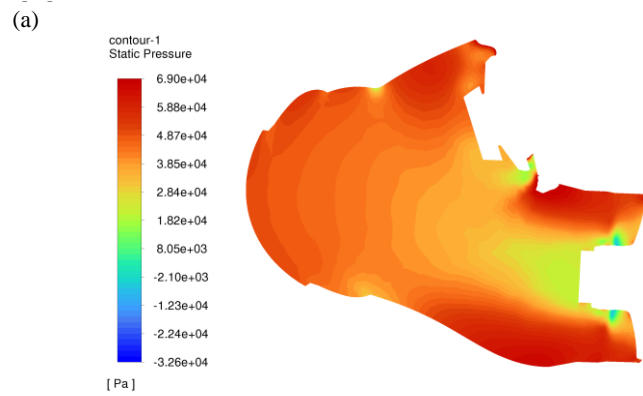
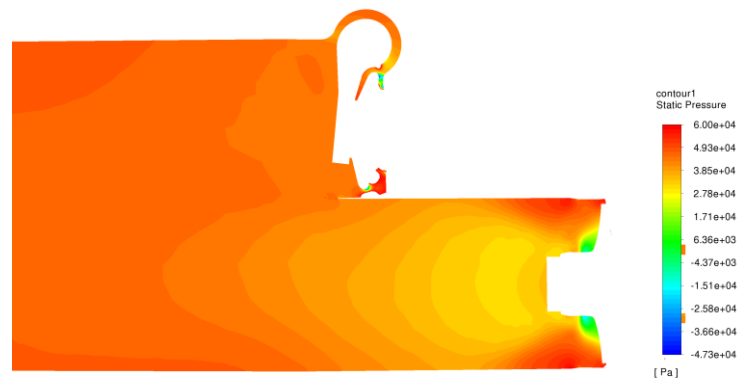


Fig. 15. 2-D static pressure contours (a) Combined Design, (b) Original design.

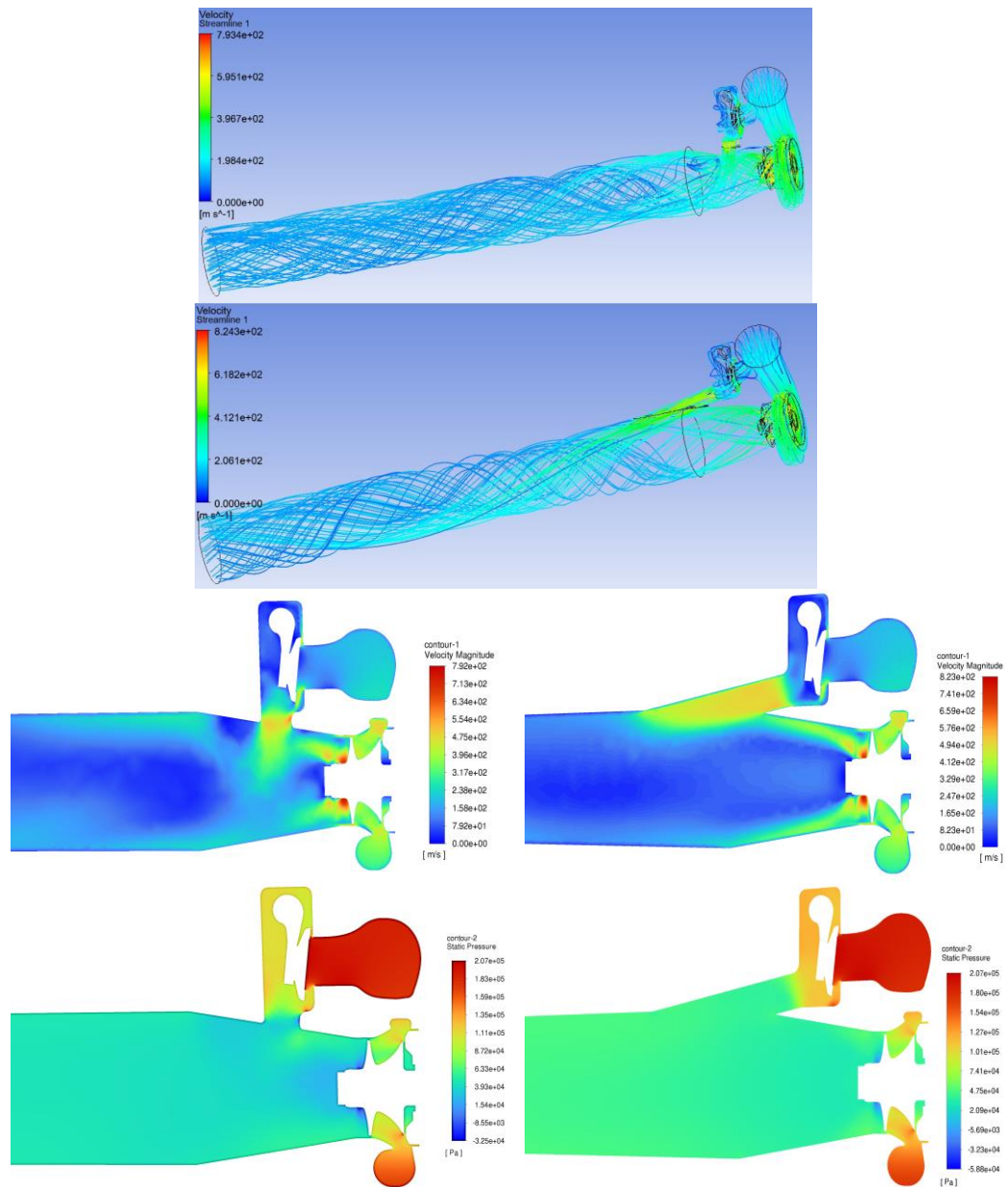


Fig. 16. Graphical results of the separated design (10° and 90°).

This shows that there is still room for more improvements to the wastegate shape and the shape of the housing around it.

Concerning the separated designs, the results reveal that there is a logarithmic increase in efficiency and useful power that is a result of decreasing the mixing angle. Figure 16 demonstrates some of the graphical results of the separated designs with 10° and 90° mixing angles. Their flow field, useful power, and efficiency can be analyzed the same way it was done for the comparison of geometries 1 and 10. It is anticipated that the efficiency and useful power of a separated design with 0° mixing angle be even greater than those of the combined design, given the fact that there are almost no vortices (deriving from the poor positioning of the wastegate) where the separated and bulk flows are reintroduced, and hence mixing losses will be less in this design. A separated

design with 0° mixing angle, however, is not more favorable than the combined design in regard of manufacturability.

The above pressure contours illustrate the whole domain.

For the jet pump design, Fig. 11 shows results that are not in agreement with the outcomes of the study undertaken by [Steglich *et al.* \(2020\)](#). This does not mean that what was deduced by them (better efficiency of the jet pump adjustable nozzle) is wrong, but it is due to the poor design of the walls of the adjustable nozzle in the current work. Figure 17 shows the visual results of these two models. Although the bypassed and bulk flow directions are somehow parallel where they are reintroduced, the bent walls of the turbine immediately in front of the wheel cause a little blockage. Besides, the protrusion of the nozzle wall in the adjustable nozzle causes

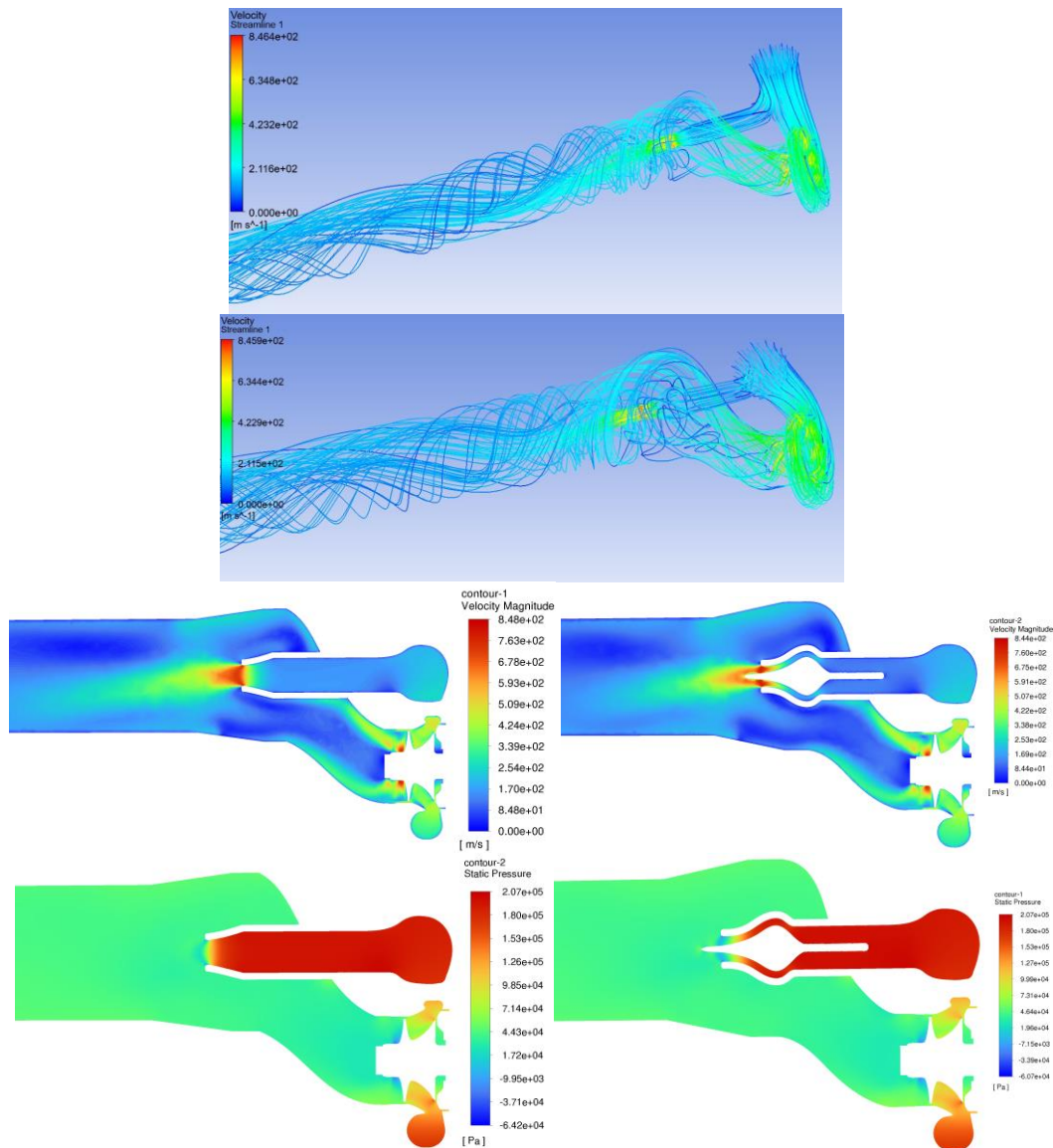


Fig. 17. Visual results of the jet pump nozzle models.

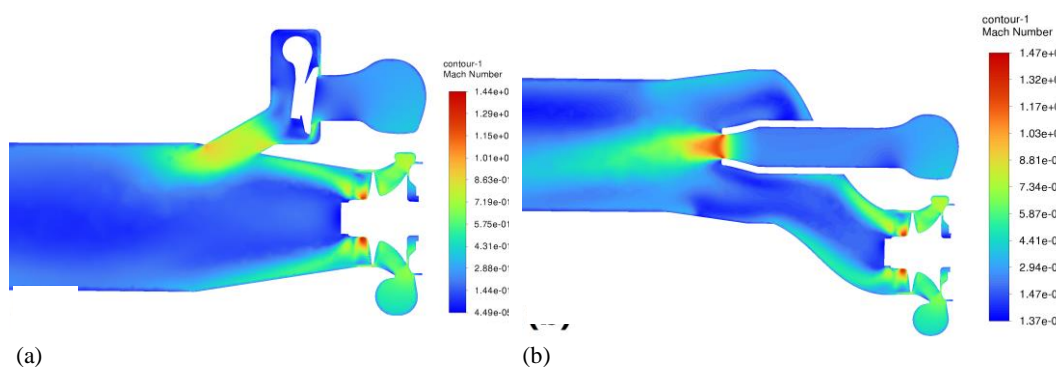


Fig. 18. Mach number contours (a) Separated 30°, (b) Jet pump fixed nozzle.

disturbance in the flow field and streamlines. By minimizing the undesirable effects of the elbow-shaped diffuser and protruded nozzle walls, the efficiency of these models has the potential to surge.

Another intriguing point about the simulations is that the bypassed flow was choked in all the models except the separated designs. This implies that the

shape of the wastegate and the housing around it plays a key role in averting or causing shocks. The analysis of the pros and cons of choking is not among the goals of this study, so they are not scrutinized any further. Figure 18 displays the Mach number in two models where the bypassed flows are choked and not choked.

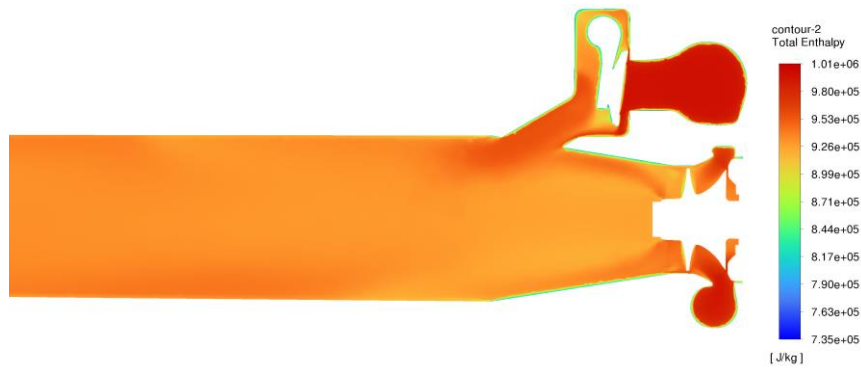


Fig. 19. Total enthalpy contours (e.g. separated 30° design).

Moreover, velocity contours and streamlines demonstrated in Fig. 12 show that as the flow develops in the outlet pipe, backflows and non-uniformity decrease. Other than that, the total enthalpy that is used for the efficiency calculation, diminishes from the inlet to the outlet (Fig. 19). For the development of two-stage turbocharger turbines, it is imperative to design the bypass and wastegate in a way that the total enthalpy does not fall significantly before the second stage.

5. CONCLUSION

The main purpose of this article was to exploit CFD in order to observe the influences of a turbocharger turbine bypass and wastegate geometry modifications on the efficiency and the flow field. The results uncovered that the mixing angle between the bypassed and turbine flows performs a crucial part in determining those outputs and the best ones are obtained when the two mentioned flows are parallel. This is because in that case, the high-velocity bypassed gas does not create an aerodynamic blockage in the way of the bulk flow (turbine flow). Therefore, it does not cause stagnation decreasing the ER and the efficiency. It is clearly concluded that any bent or elbow-shaped walls right ahead of the turbine wheel reduces the ER and the efficiency. Those two points were the primary reasons why the efficiency and the useful power increased from 39.49% and 3396.76 W in the original design to 47.38% and 3625.93 W in the novel proposed design. The shape of the wastegate and how it is positioned in the housing is not ineffectual as well. Given the fact that the regions with vortices behind the wastegate impact the stage efficiency, it is beneficial that curvy aerodynamically-efficient parts be substituted for the sharp edges and flat flaps. The aforementioned outcomes are associated with one working point at which the wastegate opening angle of the original geometry (whose experimental results were used for validation and boundary conditions of the simulations) is at its maximum amount (7 degrees) and the most turbulent flow field exists. It is indispensable for turbocharger developers to carry out simulations at several working points, including wastegate-closed conditions and opening angles of more than 7 degrees, to achieve a more

comprehensive conclusion about the turbocharger turbine performance.

REFERENCES

- Alaviyoun, S., M. Ziabasharhagh and A. Mohammadi (2022). A three-dimensional conjugate heat transfer model of a turbocharger turbine housing. *Iranian Journal of Science and Technology* 46, 71-84.
- Alaviyoun, S., M. Ziabasharhagh and M. Farajpour (2020). Experimental investigation and numerical simulation of gas flow through wastegated turbine of gasoline turbocharger. *Journal of Applied Fluid Mechanics* 13(6), 1835-1845.
- Baines, N. C. (2005). *Fundamentals of Turbocharging*. White River Junction, Vermont: Concepts NREC, USA.
- Benajes J., J. Galindo, P. Fajardo and R. Navarro (2014). Development of a segregated compressible flow solver for turbomachinery simulations. *Journal of Applied Fluid Mechanics* 7(4), 673-682.
- Capiluppi, C. (2012). *Three Dimensional CFD Simulation of a Turbocharger Turbine for Motorsport Applications*, 1st ed. M. Sc Thesis, University PARMA, Italy.
- Chen, Q., J. Ni, X. Shi, Q. Wang, Q. Chen and S. Liu (2016). Research on effect of wastegate diameter on turbocharged gasoline engine performance. *SAE Technical Paper*.
- Cox, G. (2015). *Challenges in the Design of Radial Turbines for Small Gasoline Engines*. PCA Engineers Limited, Lincoln, United Kingdom.
- Dupuis, A., V. Colliot, S. Dessarthe, D. Jeckel, L. Toussaint and A. Laurent (2014). Key features of the turbocharged engine system for the new psa 1.2l puretech e-thp 3 cylinder gasoline engine. In *19th Supercharging Conference*, Dresden, Germany.
- Fogarty, K. (2013) *Turbocharger Turbines: an Experimental Study on the Effects of Wastegate Size and Flow Passage Design*. M. Sc. Thesis,

- Department of mechanical engineering, Ohio State University, United States.
- Galindo, J., S. Hoyas, P. Fajardo and R. Navarro (2013). Set-up analysis and optimization of CFD simulations for radial turbines. *Engineering Applications of Computational Fluid Mechanics* 7(4), 441-460.
- Galindo, J., J. R. Serrano, L. M. García-Cuevas and N. Medina (2022). Twin-entry turbine losses: An analysis using CFD data. *International Journal of Engine Research* 23(7), 1180-1200.
- Gao, J., C. Ma, S. Xing, L. Sun and J. Liu (2016). Polycyclic aromatic hydrocarbon emissions of non-road diesel engine treated with non-thermal plasma technology. *Korean Journal of Chemical Engineering* 33(12), 3425-3433.
- Getzlaff, U., S. Hensel and S. Reichl (2010). Simulation of the thermo characteristics of a water-cooled turbocharger. *MTZ Worldwide* 71(9), 28-31
- Hajilouy-Benisi, A., M. Rad and M. Shahhosseini (2009). Flow and performance characteristics of twin-entry radial turbine under full and extreme partial admission conditions. *Archive of Applied Mechanics* 79(12), 1127-1143.
- Hasler, C. (2018). Optimisation of wastegated bypass flow reintroduction for increased turbine stage efficiency. In *13th International Conference on Turbocharges and Turbocharging*, London, United Kingdom.
- Hiereth, H. and P. Prenzinger (2007). *Charging the Internal Combustion Engine*. Springer-Verlag Wien, Austria.
- Marelli, S. and M. Capobianco (2011). Steady and pulsating flow efficiency of a waste-gated turbocharger radial flow turbine for automotive application. *Energy* 36(1), 459-465.
- Mosca, R., S. M. Lim and M. Mihaescu (2021, December). Influence of pulse characteristics on turbocharger radial turbine. *Journal of Engineering for Gas Turbines and Power* 144(2), 021018.
- Mousavi, S., A. Nejat, S. Alaviyoun and M. Nejat (2021). An integrated turbocharger matching program for internal combustion engines. *Journal of Applied Fluid Mechanics* 14(4), 1209-1222.
- Newton, P., C. Copeland, R. Martinez-Botas and M. Seiler (2012). An audit of aerodynamic loss in a double entry turbine under full and partial admission, *International Journal of Heat and Fluid Flow* 33(1), 70-80.
- Rezk, A., S. Sharma, S. Barrans, A. K. Hossain, S. P. Lee and M. Imran (2021). Computational study of a radial flow turbine operates under various pulsating flow shapes and amplitudes. *Journal of Energy Resources Technology* 143(12), 120904.
- Salehi, R., G. Vossoughi and A. Alasty (2013). Modeling and estimation of unmeasured variables in a wastegate operated turbocharger. *ASME Journal of Engineering for Gas Turbines and Power* 136 (5), 052601.
- Salim W. (2014). *Study of Externally Waste-Gated Turbine Performance under Steady and Pulsating Inlet Conditions for Improved Turbocharger Matching*. Ph. D. Thesis, Department of Mechanical Engineering, Imperial College London, United Kingdom.
- Serrano, J. R., F. J. Arnau, T. Andres and V. Samala (2017). Experimental procedure for the characterization of turbocharger's waste-gate discharge coefficient. *Advances in Mechanical Engineering* 9(10), 1-9.
- Shah, S. P., S. A. Channiwala, D. B. Kulshreshtha and G. Chaudhari (2016). Study of flow patterns in radial and back swept turbine rotor under design and off-design conditions. *Journal of Applied Fluid Mechanics* 9(4), 1791-1798.
- Siggeirsson, E. and S. Gunnarsson. (2015). *Conceptual Design Tool for Radial Turbines*. M. Sc. Thesis, Department of Applied Mechanics, Chalmers University of Technology, Gothenburg, Sweden.
- Steglich, T., M. Vogt and M. Weiss (2020). Alternative bypass control for turbochargers. *MTZ Worldwide* 81, 46-51.
- Tabatabaei, H., M. Boroomand and M. Taeibi Rahni (2012). An investigation on turbocharger turbine performance parameters under inlet pulsating flow. *Journal of Fluids Engineering* 134(8), 081102-081110.
- Wibmer, M., T. Schmidt, O. Grabherr and B. Durst (2015). Simulation of turbocharger wastegate dynamics. *MTZ Worldwide* 76, 28-31.
- Yang, M., L. Pan, M. Shu, K. Deng, Z. Ding and Y. Tian (2021). Aerodynamic interaction of turbines in a regulated two-stage turbocharging system. *Proceedings of the Institution of Mechanical Engineers, Part D: Journal of Automobile Engineering*. 236(13), 2961-2973.
- Zhao, R., W. Zhuge, Y. Zhang, M. Yang and R. Martinez Botas (2016). Numerical study of a two-stage turbine characteristic under pulsating flow conditions. *Journal of Mechanical Science and Technology* 30(2), 557-565.